COMMENTARY

# Spectral imaging fluorescence microscopy

**Tokuko Haraguchi[1,2], Takeshi Shimi[1,2], Takako Koujin[1], Noriyo Hashiguchi[1] and Yasushi Hiraoka[1,2,*]**

[1]*CREST Research Project, Kansai Advanced Research Center, Communications Research Laboratory, 588-2 Iwaoka, Iwaoka-cho, Nishi-ku, Kobe 651-2492, Japan*

[2]*Department of Biology, Graduate School of Science, Osaka University, 1-1 Machikaneyama, Toyonaka, Osaka 560-0043, Japan*

**The spectral resolution of fluorescence microscope images in living cells is achieved by using a confocal laser scanning microscope equipped with grating optics. This capability of temporal and spectral resolution is especially useful for detecting spectral changes of a fluorescent dye; for example, those associated with fluorescence resonance energy transfer (FRET). Using the spectral imaging fluorescence microscope system, it is also possible to resolve emitted signals from fluorescent dyes that have spectra largely overlapping with each other, such as fluorescein isothiocyanate (FITC) and green fluorescent protein (GFP).**

Since the discovery of the jellyfish green fluorescent protein (GFP) and its colour variants, multiple wavelength fluorescence imaging has become a useful tool in studies of cell biology. For imaging multiple wavelength fluorescence images, computer-controlled microscope systems that automatically switch optical filters during observation have been developed (Hiraoka *et al*. 1991; Haraguchi *et al*. 1999). While such microscope systems can collect fluorescence images at multiple wavelengths, fluorescence emissions with a spectral overlap can cause cross-talk between the emitted signals, thus limiting the choice of fluorescent dyes.

Here we introduce a microscope technique that is capable of resolving the spectra of fluorescence images without switching optical filters; the fluorescence spectra are obtained as a series of images as a function of fluorescence wavelength. This capability of spectral resolution makes it possible to unmix the cross-talk between overlapping fluoresence emissions. It also provides a unique capability for detecting spectral changes in fluorescent indicators; for example, an indicator for fluorescence resonance energy transfer (FRET). Such techniques have been devised by the use of an acousto-optic tunable filter (AOTF) or a grating (Wachman *et al*. 1997; Hanley *et al*. 2000; Tsurui *et al*. 2000; Ford *et al*. 2001; Lansford *et al*. 2001).

*Correspondence*: E-mail: yasushi@crl.go.jp

The hardware design we used is an implementation of the previously reported technology of two-photon imaging spectroscopy (Lansford *et al*. 2001) to a commercial single-photon confocal scanning microscope; the technology is applicable to a single-photon or multiphoton fluorescence microscope. In this spectral imaging microscope system (LSM510 META; Carl Zeiss, Jena, Germany), fluorescence spectra are resolved using grating optics; resolved fluorescence spectra at each pixel are detected by an array of 32 photomultiplier tubes (PMT) placed at the confocal plane, and recorded on a pixel-by-pixel basis during scanning to generate a set of images, each corresponding to the fluorescence wavelength resolved at 10 nm intervals. The maximum range of wavelength is 380–720 nm, resolved to 32 divisions.

## Spectral resolution of fluorescence images

We first demonstrate that the use of grating optics allows us to obtain multiple-wavelength images without switching optical filters. An example of spectral imaging, or imaging spectroscopy, is shown in Fig. 1A. A mixture of four fluorescent beads emitting light of different wavelengths (515 nm, 560 nm, 605 nm and 645 nm; see legend to Fig. 1) was observed. Figure 1A shows a set of 20 spectral images ranging from 485 to 688 nm, and Fig. 1B shows selected images at 417 nm, 570 nm, 602 nm and 656 nm. Figure 1C shows spectra for each of the four beads. These beads have distinct spectral

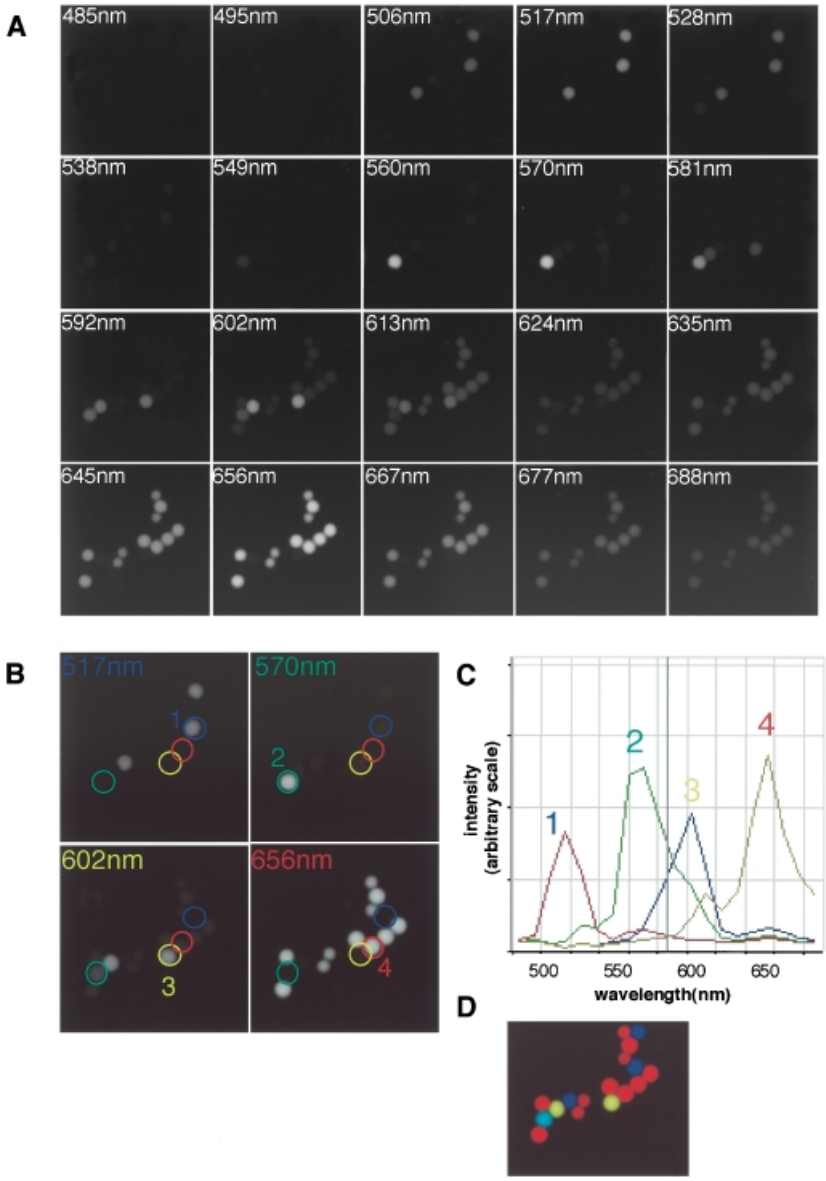


**Figure 1** Spectral imaging. (A) Spectal images of fluorescent beads. Four different fluorescent beads of 1 μm diameter were mixed: wavelengths for excitation/emission were: 490/515 nm, 530/560 nm, 580/605 nm and 625/645 nm (Molecular Probes, Eugene, OR). Beads were excited by 488 nm and 543 nm light from an argon laser, and 633 nm light from a helium-neon laser. A series of images were obtained on Zeiss LSM510 META using a water-immersion objective lens (C-Apochromat 40×/NA = 1.2) and a dichroic mirror (HFT UV/488/543/633). (B) Images of beads at selected wavelengths. (C) Spectra of the beads. (D) Colour separation of the four fluorescent beads.

profiles, and can thus be separated without further processing. Figure 1D shows a pseudocolour representation of the beads.

This capability of spectral imaging makes it possible to resolve the fluorescence images of dyes that have a large spectral overlap of fluorescence emission. The fluorescence spectra of an observed image is a linear combination of the spectra of multiple fluorescent dyes used to stain the specimen. By knowing the fluorescence spectra of each of the dyes, observed mixed spectra can be unmixed to each component; this calculation is generally called 'linear unmixing' (Lansford *et al.* 2001). Such processing of the observed image on a pixel-by-pixel basis produces a set of spectrally resolved images. Figure 2 shows an example of colour separation of GFP and fluorescein isothiocyanate (FITC) in fixed HeLa cells. Because the fluorescence of GFP and FITC is separated by only 7 nm at their emission peak, images of GFP and FITC are not resolved using a standard filter combination for the GFP/FITC wavelength. A set of spectral images were obtained for these cells (Fig. 2A), and the fluorescence spectra of GFP and FITC measured at the regions labelled 1 and 2, respectively (Fig. 2B). Using these spectra as a reference spectrum for each dye, the observed spectral images were processed to resolve FITC and GFP images by a linear unmixing algorithm (Fig. 2C).

 

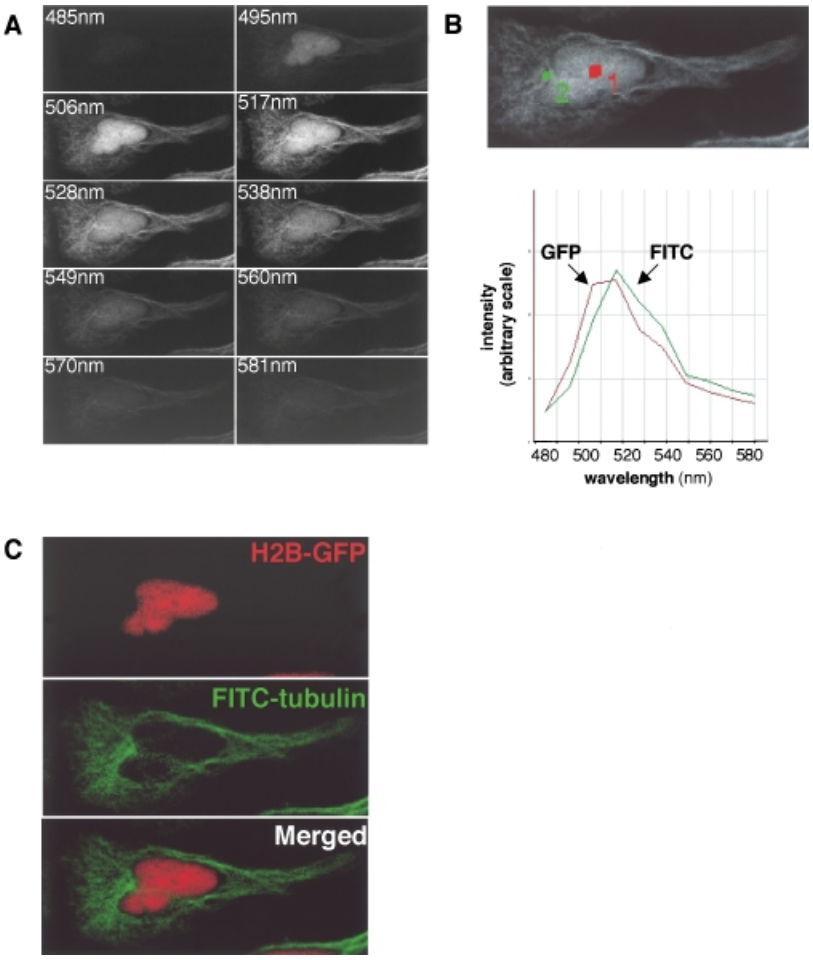


**Figure 2** Colour separation of GFP and FITC. HeLa cells expressing GFP-fused histone H2B (Kanda *et al*. 1998) were fixed with ice-cold methanol for 15 min; microtubules were stained with the anti-α tubulin antibody TAT1 and FITC-labelled secondary antibody. The specimen was excited by 488 nm light from an argon laser. (A) A series of images were obtained using a water-immersion objective lens (C-Apochromat 40×/NA = 1.2) and a dichroic mirror (HFT488). (B) Regions in the image that were stained with only one of the dyes were selected and the spectrum measured at this selected region and used as the reference spectrum for the dye in question. (C) Images were processed by a linear unmixing algorithm using the reference spectrum of each dye. The merged image with pseudocolours is shown in the bottom panel.

Figure 3 shows another example of the colour separation of GFP and yellow fluorescent protein (YFP) in HeLa cells (see legend to Fig. 3 for details). Thus, the linear unmixing demonstrates a colour separation of fluorescence images with a large spectral overlap such as GFP and FITC, or GFP and YFP, as an extreme example.

## Spectral images of living cells

Spectral imaging provides an opportunity for rapidly recording multiple wavelength images with no need for switching optical filters. This capability is especially useful in time-lapse observations of living cells. The spectral imaging of living cells produces a temporal series of spectral images, as shown in Fig. 4A. In this example, the nuclear membrane was stained with lamin B receptor (LBR) protein with cyan fluorescent protein (CFP) (Haraguchi *et al*. 2000), and protein import into the nucleus was detected using YFP fused to the protein STAT1 (signal transducer and activator of transcription). STAT1 is usually distributed in the cytoplasm, and enters the nucleus following treatment with γ-interferon (Köster & Hauser 1999; Sekimoto *et al*. 1997). This example demonstrates the spectral and temporal resolution of fluorescently stained living cells; the linear unmixing of the images clearly separated the CFP staining of the nuclear membrane and YFP staining of STAT1 (Fig. 4B).

## Detection of spectral changes

The capability of this system for the temporal and spectral resolution of fluorescence microscope images provides a unique opportunity for detecting spectral changes of fluorescence in living cells. Figure 5 demonstrates an example of spectral change of a dye induced by changes in the intracellular calcium concentration in HeLa cells. In this example, we used a split version of yellow chameleon-2 (YC2.1) as a FRET-based calcium indicator dye (Miyawaki *et al*. 1999). Split YC2.1 generates FRET by interaction between calmodulin (CaM) and

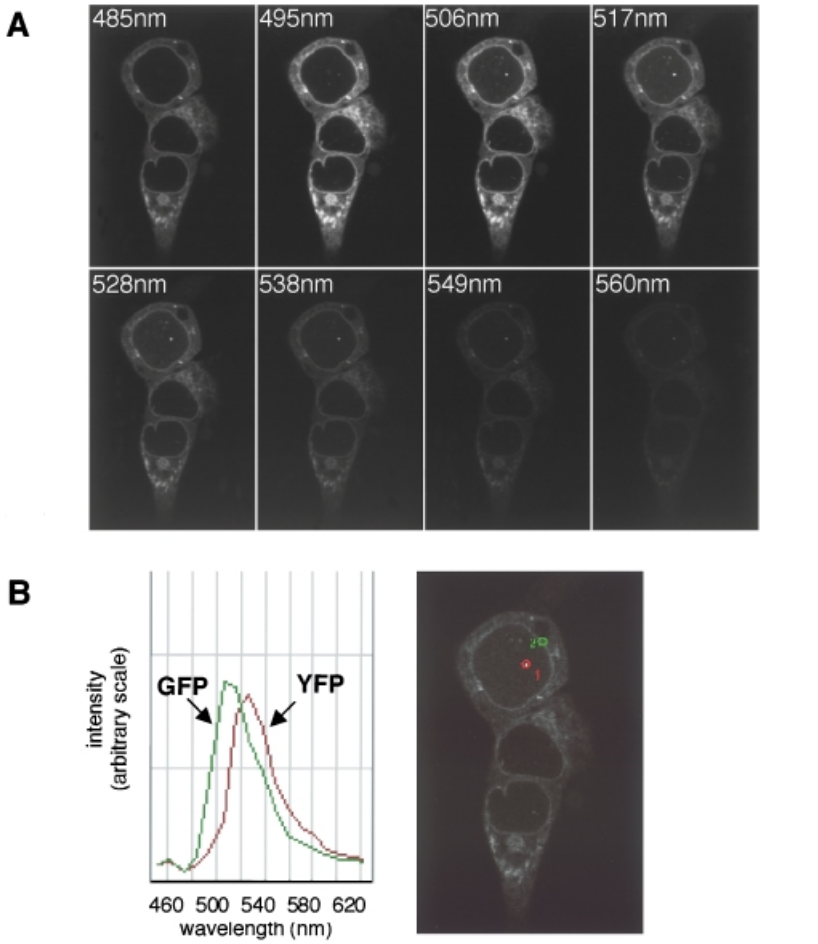


**Figure 3** Colour separation of GFP and YFP. HeLa cells expressing GFP-emerin and YFP-SUMO1 were excited by 458 nm light from an argon laser. (A) A series of images were obtained using a water-immersion objective lens (C-Apochromat 40×/NA = 1.2) and a dichroic mirror (HFT488). (B) The regions in the image that were stained with only one of the dyes were selected and the fluorescence spectra of each dye measured at the selected regions were used as a reference for spectra of each of the dyes. (C) Images were computationally processed by a linear unmixing algorithm using the reference spectrum of each dye; the merged image with pseudocolours is shown in the right panel.

M13 in the presence of $Ca^{2+}$ (Fig. 5A). To detect such a spectral change associated with FRET, CFP-CaM and M13-YFP were introduced into living HeLa cells, and the calcium uptake to the cells was induced by the addition of ionomycin. Images were obtained as a temporal series of spectral images; fluorescence intensity is displayed in Fig. 5B as a pseudocolour representation. The fluorescence of YC2.1 changed its spectra shortly after the addition of ionomycin (Fig. 5B,C). In Fig. 6C, fluorescence intensities at an exitation wavelength of 484 nm and at 527 nm are plotted as a function of time; the acceptor signal (at 527 nm) increased and the donor signal (at 484 nm) decreased following the induction, indicating that FRET occurred. In spectral imaging,

 

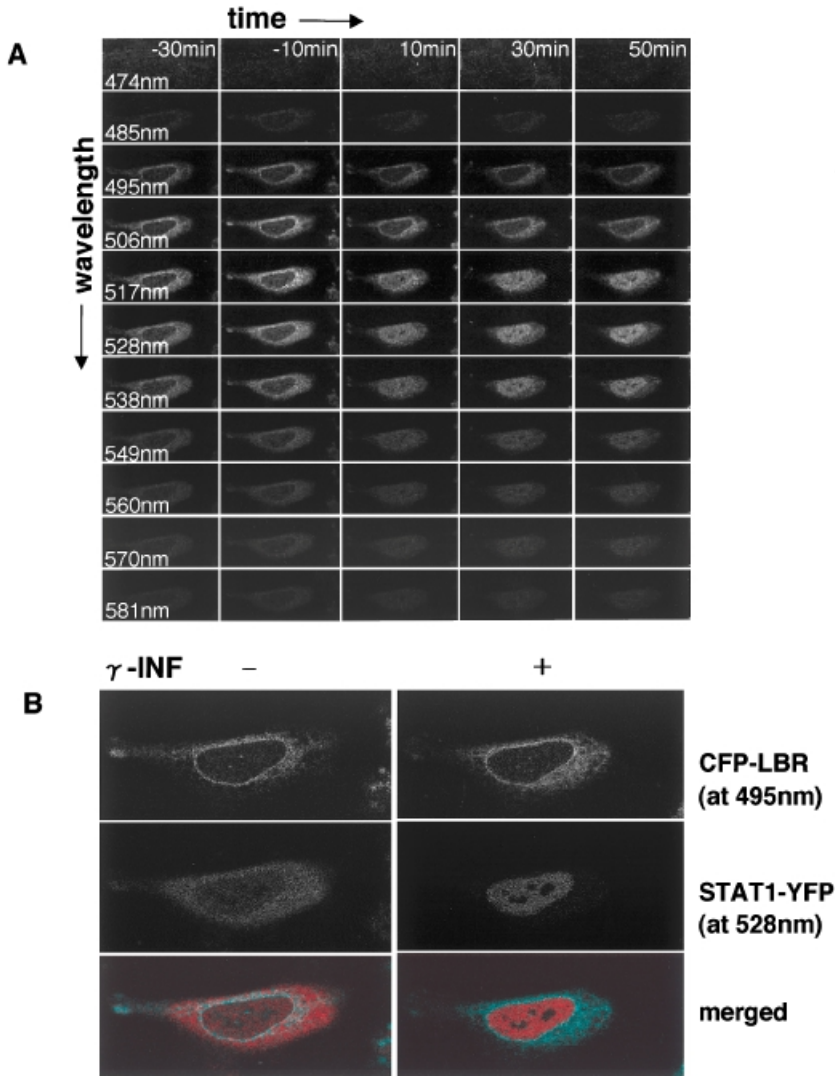


**Figure 4** Time-lapse spectral images of living cells. (A) Living HeLa cells expressing CFP fused with LBR and YFP fused with STAT1. Cells were excited by 458 nm and 477 nm light from an argon laser. Images were obtained using an oil-immersion objective lens (Plan-Apochromat 63×/NA = 1.4) and a dichroic mirror (HFT488). Live observation was carried out at 37 °C up to 24 h in 5 min intervals. A set of spectral images at each time-point are displayed in each column as a function of fluorescence wavelength, and columns of spectral images are displayed from left to right as a function of time. Numbers at the top of each column represent time in minutes after treatment with γ-interferon. (B) Selected images computationally processed by linear umixing; 10 min before and 10 min after addition of γ-interferon.

spectral changes can be measured directly at multiple wavelengths, as shown in Fig. 6A and B, whereas the fluorescence intensity measured conventionally at only two wavelengths is used to estimate FRET efficiency. Thus, spectral imaging can take full advantage of fluorescent indicator dyes that undergo spectral changes, and will provide wider applications for such fluorescent indicators.

## Concluding remarks

Spectral imaging solves some of the technological limitations that complicate multiple-wavelength imaging. In this manner, efficient multiple colour image acquisition is achieved by the use of grating optics to resolve fluorescence spectra. Using spectral imaging, it is now possible to detect the spectra of fluorescence microscope images, which has not been possible before. This capability is useful for efficiently resolving spectral cross-talk by linear unmixing computation.

Spectral imaging is best appreciated as a tool for detecting spectral changes in fluorescence, for example, those of FRET indicators. This capability will also eliminate problems associated with autofluorescence. Fluorescence staining is often interfered with by the autofluorescence of cells or tissues—especially in plants. Spectral imaging and linear unmixing can remove autofluorescence by separating its spectra from the spectra of fluorescently stained organelles and cell structures of interest.

Finally, it should be mentioned that the advent of spectral imaging will provide an impetus for the

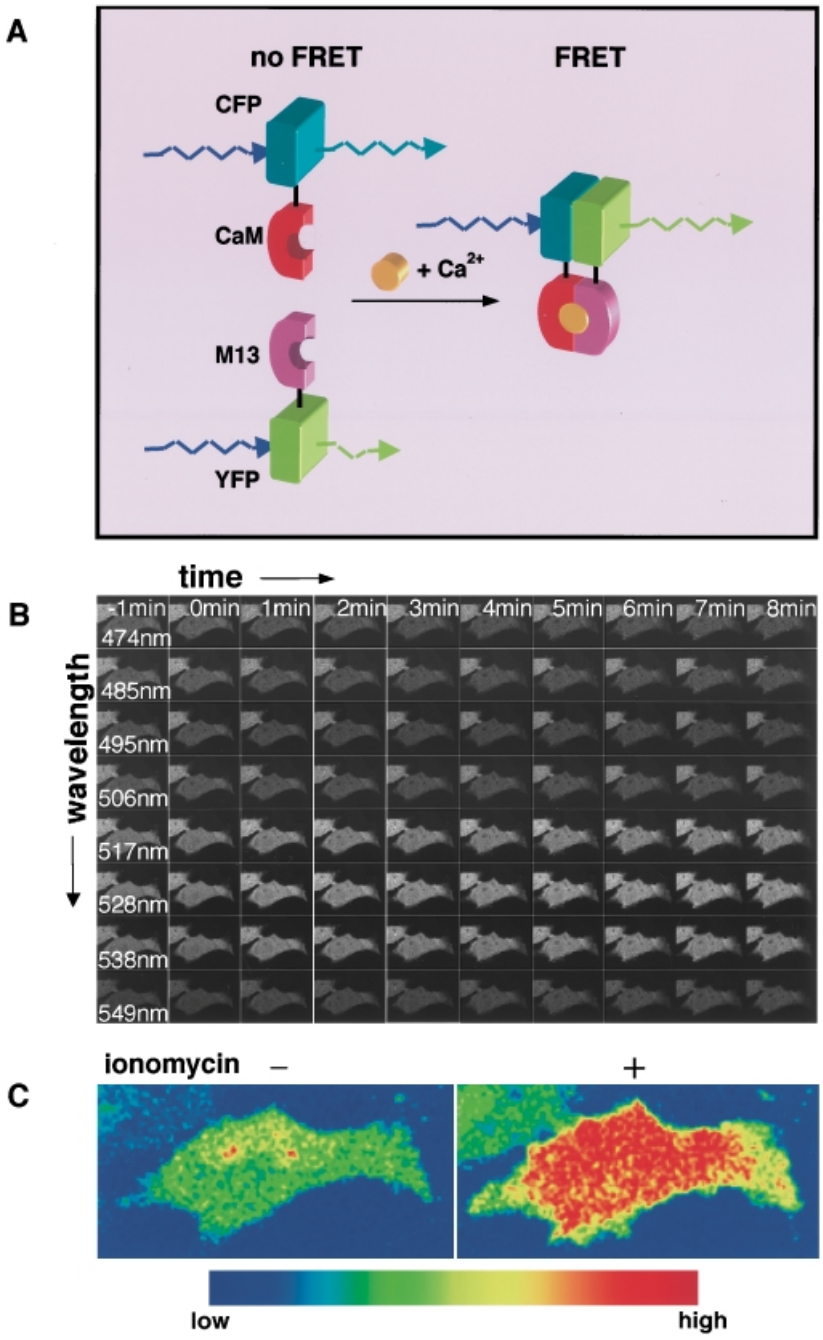


**Figure 5** FRET images of yellow chameleon-2. (A) A split version of YC2.1 is composed of two separate portions of CFP-tagged calmodulin (CFP-CaM) and YFP-tagged M13 (YFP-M13) as a donor and an acceptor of FRET, respectively (Miyawaki *et al.* 1999). The calmodulin portion (CaM) and the M13 portion interact with each other in the presence of $Ca^{2+}$ to generate FRET. (B) Living HeLa cells expressing CFP-CaM and YFP-M13 were observed using a water-immersion objective lens (C-Apochromat 40×/NA = 1.2) and a dichroic mirror (HFT488); excitation light of wavelength 458 nm was from an argon laser. (C) Ratio image of fluorescence intensity at 528 nm to that at 495 nm is displayed for before and after the addition of ionomycin. Basically the same results were obtained using a joint version of YC2.1 (CFP-CaM-M13-YFP) which generates FRET by its conformational change in the presence of $Ca^{2+}$ (Miyawaki *et al.* 1999).

development of a new class of fluorescent dyes. Currently available fluorescent dyes are not necessarily optimal for spectral imaging. Wavelength selection by optical filters requires fluorescent dyes with different wavelengths for both excitation and emission. On the other hand, for spectral imaging, dyes excited by the light of a single excitation wavelength and emitting light of separate wavelengths will be more preferable, allowing a single laser to excite multiple dyes simultaneously. Dyes that change their spectra under certain conditions (e.g. phosphorylation and dephosphorylation events, molecular interactions or conformational changes of proteins) are also awaited for applications in spectral imaging to detect changes in the intracellular environment. This methodology could therefore prove useful for the real-time detection of biochemical reactions inside single cells.

 

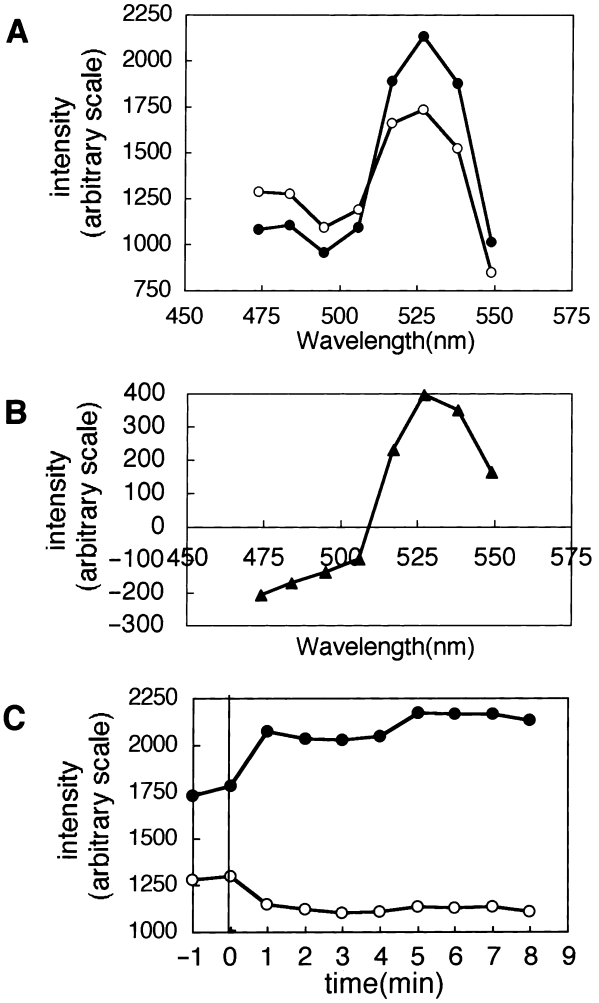


**Figure 6** Spectral change of yellow chameleon-2. (A) Fluorescence spectra of split YC2.1 before (open circle) and after (filled circle) ionomycin treatment. (B) FRET spectra, subtracting fluorescence spectra before ionomycin treatment from that after ionomycin treatment. (C) Fluorescence intensity at 488 nm and 528 nm is plotted as a function of time. Time 0 indicates the addition of ionomycin.

## Acknowledgements

We are grateful to Dr Yoshihiro Yoneda (Osaka University) for DNA plasmids encoding STAT1, and Dr Atsushi Miyawaki (Brain Science Institute, RIKEN) for the yellow chameleon dyes. This work was supported by a grant from the Japan Science and Technology Corporation to Y.H.

## References

Ford, B.K., Volin, C.E., Murphy, S.M., Lynch, R.M. & Descour, M.R. (2001) Computed tomography-based spectral imaging for fluorescence microscopy. *Biophys. J.* **80**, 986–993.

Hanley, Q.S., Verveer, P.J., Arndt-Jovin, D.J. & Jovin, T.M. (2000) Three-dimensional spectral imaging by hadamard transform spectroscopy in a programmable array microscope. *J. Microsc.* **197**, 5–14.

Haraguchi, T., Ding, D.-Q., Yamamoto, A., Kaneda, T., Koujin, T. & Hiraoka, Y. (1999) Multiple-color fluorescence imaging of chromosomes and microtubules in living cells. *Cell Struct. Funct.* **24**, 291–298.

Haraguchi, T., Koujin, T., Hayakawa, T., *et al.* (2000) Live fluorescence imaging reveals early recruitment of emerin, LBR, RanBP2, and Nup153 to reforming functional nuclear envelopes. *J. Cell Sci.* **113**, 779–794.

Hiraoka, Y., Swedlow, J.R., Paddy, M.R., Agard, D.A. & Sedat, J.W. (1991) Three-dimensional multiple-wavelength fluorescence microscopy for the structural analysis of biological phenomena. *Semin. Cell Biol.* **2**, 153–165.

Kanda, T., Sullivan, K.F. & Wahl, G.M. (1998) Histone-GFP fusion protein enables sensitive analysis of chromosome dynamics in living mammalian cells. *Curr. Biol.* **8**, 377–385.

Köster, M. & Hauser, H. (1999) Dynamic redistribution of STAT1 protein in IFN signaling visualized by GFP fusion proteins. *Eur. J. Biochem.* **260**, 137–144.

Lansford, R., Bearman, G. & Fraser, S.E. (2001) Resolution of multiple green fluorescent protein color variants and dyes using two-photon microscopy and imaging spectroscopy. *J. Biomed. Optics* **6**, 311–318.

Miyawaki, A., Griesbeck, O., Heim, R. & Tsien, R.Y. (1999) Dynamic and quantitative $Ca^{2+}$ measurements using improved cameleons. *Proc. Natl. Acad. Sci. USA* **96**, 2135–2140.

Sekimoto, T., Imamoto, N., Nakajima, K., Hirano, T. & Yoneda, Y. (1997) Extracellular signal-dependent nuclear import of Stat1 is mediated by nuclear pore-targeting complex formation with NPI-1, but not Rch1. *EMBO J.* **16**, 7067–7077.

Tsurui, H., Nishimura, H., Hattori, S., Hirose, S., Okumura, K. & Shirai, T. (2000) Seven-color fluorescence imaging of tissue samples based on Fourier spectroscopy and singular value decomposition. *J. Histochem. Cytochem.* **48**, 653–662.

Wachman, E.S., Niu, W. & Farkas, D.L. (1997) AOTF microscope for imaging with increased speed and spectral versatility. *Biophys. J.* **73**, 1215–1222.